Journal of Zhejiang University SCIENCE A
ISSN 1673-565X (Print); ISSN 1862-1775 (Online)
www.zju.edu.cn/jzus; www.springerlink.com
E-mail: jzus@zju.edu.cn

Classification of power quality combined disturbances based on phase space reconstruction and support vector machines*

Zhi-yong LI, Wei-lin WU‡
(*School of Electrical Engineering, Zhejiang University, Hangzhou 310027, China*)
E-mail: zhiyongrwx_jill@163.com; eewuwl@zju.edu.cn
Received May 21, 2007; revision accepted Aug. 10, 2007

Abstract: Power Quality (PQ) combined disturbances become common along with ubiquity of voltage flickers and harmonics. This paper presents a novel approach to classify the different patterns of PQ combined disturbances. The classification system consists of two parts, namely the feature extraction and the automatic recognition. In the feature extraction stage, Phase Space Reconstruction (PSR), a time series analysis tool, is utilized to construct disturbance signal trajectories. For these trajectories, several indices are proposed to form the feature vectors. Support Vector Machines (SVMs) are then implemented to recognize the different patterns and to evaluate the efficiencies. The types of disturbances discussed include a combination of short-term disturbances (voltage sags, swells) and long-term disturbances (flickers, harmonics), as well as their homologous single ones. The feasibilities of the proposed approach are verified by simulation with thousands of PQ events. Comparison studies based on Wavelet Transform (WT) and Artificial Neural Network (ANN) are also reported to show its advantages.

Key words: Power Quality (PQ), Combined disturbance, Classification, Phase Space Reconstruction (PSR), Support Vector Machines (SVMs)
doi:10.1631/jzus.A071261 **Document code:** A **CLC number:** TM711

INTRODUCTION

Data storage capability of Power Quality (PQ) monitors has been advanced significantly in the past few years. This development results in the tremendous amount of data accumulated with useful but hidden information. Meanwhile, the contamination of PQ environment is getting worse because extensively applied power electronic technologies lead to a wide diffusion of nonlinear, time-variant loads in power distribution network. In this context, detecting and recognizing PQ disturbances from PQ raw data are necessary. By identifying the causes and sources of such disturbances, their effects can be neutralized by using suitable corrective and preventive measures.

So far, great efforts have been made for solving this signal processing and knowledge discovery problem (Gaouda *et al*., 2001; Tiwari and Shukla, 2002; Chilukuri and Dash, 2004; Chilukuri *et al*., 2004; Liao and Lee, 2004; Wang and Mamishev, 2004; Youssef *et al*., 2004; Abdel-Galil *et al*., 2005; Chen, 2005; Germen *et al*., 2005; He and Starzyk, 2006; Tong *et al*., 2006; Axelberg *et al*., 2007; Li and Wu, 2007). However, most of them dealt with PQ single disturbances only. Few of them considered the harmonic-related combined ones (Gaouda *et al*., 2001; He and Starzyk, 2006). As we know, none of the existing works reported the classification performance of flicker-related combined disturbances. It is challenging to classify the different kinds of combined disturbances.

In recent years, many electric devices like nonlinear loads, including adjustable speed drives, UPS, switch mode power converters, microprocessor controls, robotics, fax machines, laser printers and so on have been widely applied to industry and dwelling,

‡ Corresponding author
* Project (No. 50437010) supported by the Key Program of the National Natural Science Foundation of China

which feature with the nonlinear loads and inject harmonic currents into power grid and distort the voltage waveform all the time. In some places, the installation of reciprocating compressors, electric furnaces or dispersed generations cause periodic voltage fluctuations. These two long-term PQ disturbances exist permanently in distribution network and combine with short-term disturbances such as voltage sags or swells.

Categorizing these combined disturbances into a single group will lead to an inaccurate analysis. The existence of short duration voltage variations confuses spectrum analysis of harmonic voltage waveform, or temporarily exaggerates the severity of voltage flicker. Besides, it is impossible to record the short-term disturbances completely since they may be concealed by the permanent distortion. For solving these problems, this paper presents a novel classification system with the capability of recognizing combined disturbances.

A classification system always comprises two sequential processes: a feature extraction and an automatic recognition. In the feature extraction stage, Wavelet Transform (WT) is widely used to construct feature vectors for subsequent training and testing (Gaouda *et al*., 2001; Tiwari and Shukla, 2002; Liao and Lee, 2004; Abdel-Galil *et al*., 2005; Chen, 2005; Germen *et al*., 2005; He and Starzyk, 2006; Tong *et al*., 2006). Besides, several other mathematical manipulations are adopted, such as Fourier transform (Liao and Lee, 2004; Wang and Mamishev, 2004; Abdel-Galil *et al*., 2005; Chen, 2005), S-transform (Chilukuri and Dash, 2004; Chilukuri *et al*., 2004) and Walsh transform (Youssef *et al*., 2004). For classifier design, the pattern recognition methods including fuzzy logic (Tiwari and Shukla, 2002; Chilukuri and Dash, 2004; Liao and Lee, 2004), hidden Markov models (Abdel-Galil *et al*., 2005), rule table (Gaouda *et al*., 2001; Chilukuri *et al*., 2004), Artificial Neural Network (ANN) (Wang and Mamishev, 2004; Tong *et al*., 2006), self-organizing map (Germen *et al*., 2005), dynamic time warping (Youssef *et al*., 2004) and Support Vector Machines (SVMs) (Axelberg *et al*., 2007; Li and Wu, 2007), have been studied and proved feasible.

On the basis of (Li and Wu, 2007), this paper builds an improved classification system for PQ combined disturbances based on Phase Space Reconstruction (PSR) and SVMs. Unlike the existing feature extraction tools which map waveform information from time domain into frequency domain, the PSR-based approach carries out image processing and defines features without mathematical transform. Features extracted from PSR trajectories prove more effective than that from spectral characteristics to recognize flicker-related combined disturbances. By exploiting the sparseness of the solution, the convexity of the optimization problem and implicit mapping into feature space, SVMs can realize statistical classification with remarkable computational efficiency. Subsequent simulations show that the proposed system can achieve a satisfying performance.

The rest of this paper is organized as follows. Sections 2 and 3 discuss the feature extraction and the automatic recognition, respectively. Section 2 introduces the basic concepts of PSR and illustrates how to extract disturbance features using PSR. Section 3 presents the concept and scheme of SVM classifier. In Section 4, the data generation and simulation results are given for verifying the proposed system. Comparison studies and discussions are also reported. Finally, Section 5 draws the conclusion.

PSR-BASED FEATURE EXTRACTION

Basic theory of PSR

PSR was first utilized to reconstruct the motion on strange attractors in chaotic systems. Borrowing the idea of constructing signal trajectories from time series, Li and Wu (2006) introduced PSR into PQ research field.

The basic theory of PSR is to convert a scalar sequence of measurements into state vectors. The values of variables at a certain moment and those values after τ, 2τ, …, $(m-1)\tau$ time intervals are treated as coordinates of a special point in m-dimensional phase space. Thus, for a single variable sequence x_1, x_2, …, x_N, a delay reconstruction in m dimensions can be formed by the vector $\boldsymbol{X}_i$, given as

$$\boldsymbol{X}_i = [x_i, x_{i+\tau}, \ldots, x_{i+(m-2)\tau}, x_{i+(m-1)\tau}], \qquad (1)$$

where i=1, 2, …, L and L=1, 2, …, $N-(m-1)\tau$.

From Eq.(1), we get the value matrix that carries the coordinates of points which form the trajectory of

$$\begin{cases} \boldsymbol{X}_1 = [x_1, x_{1+\tau}, \ldots, x_{1+(m-1)\tau}], \\ \boldsymbol{X}_2 = [x_2, x_{2+\tau}, \ldots, x_{2+(m-1)\tau}], \\ \quad \vdots \\ \boldsymbol{X}_L = [x_L, x_{L+\tau}, \ldots, x_{L+(m-1)\tau}]. \end{cases} \tag{2}$$

Take the sinusoidal sequence as an example. From a normalized sine waveform with 50 Hz power frequency (Fig.1a), which is sampled at 4800 Hz, we obtain time series of 96 points for every period:

$$[x_1, x_2, \ldots, x_{96}] = [0, 0.065, 0.013, \ldots, 0.998, 1, 0.998, \ldots, -0.013, -0.065]. \tag{3}$$

We construct the trajectory in 2D phase plane (m=2, τ=20). The values of x_i and x_{i+20} indicate the position of the ith point in trajectory.

$$\begin{cases} \boldsymbol{X}_1 = [x_1, x_{21}] = [0, 0.966], \\ \boldsymbol{X}_2 = [x_2, x_{22}] = [0.066, 0.981], \\ \quad \vdots \\ \boldsymbol{X}_{96} = [x_{96}, x_{116}] = [x_{96}, x_{30}] = [-0.065, 0.947]. \end{cases} \tag{4}$$

Then, a sequence sampled from sine wave in a period can be mapped into 96 points which compose a sinusoidal trajectory shown in Fig.1b.

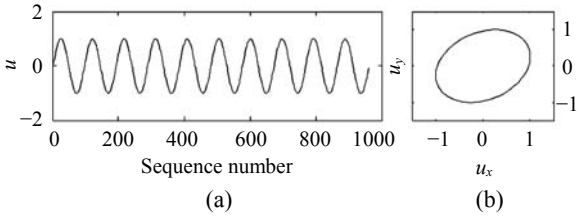

Fig.1 A pure sine wave (a) and its corresponding trajectory (b) using Phase Space Reconstruction (PSR)

Figs.2 and 3 depict the PSR process of harmonic and flicker waveforms, respectively. These two PSR trajectories look to be distorted and obviously differ from each other. In the next part, we further illustrate how to extract discriminative features from those trajectories for machine learning and recognition.

Feature extraction

1. Image processing

As shown in Fig.1b, in a per-unit system the trajectory of sine wave is restricted to the square

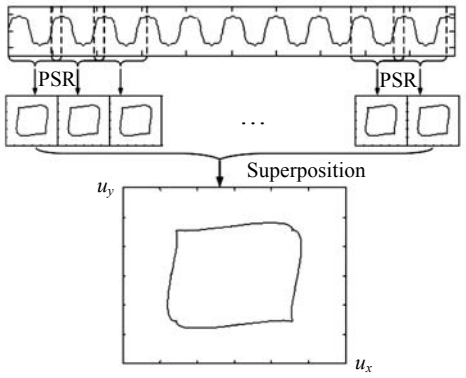

Fig.2 PSR process of harmonic waveform

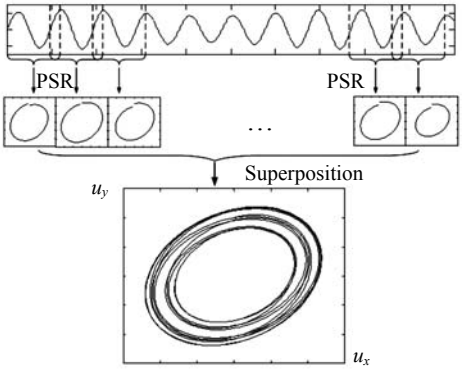

Fig.3 PSR process of flicker waveform

$[-1, 1]\times[-1, 1]$. Taking a potential over-voltage into account, we pick a larger area of $[-1.5, 1.5]\times[-1.5, 1.5]$ for further analysis. This area is divided into 300×300 segments. Each segment indicates a 2-value pixel (black pixel: 1; white pixel: 0). The pixels are assigned 1 if any point of the trajectory falls into the corresponding segment, and the remnant pixels remain 0. After such encoding process, the graph in Fig.1b will be transformed into a binary image.

In such an image, the power system voltage waveform can be regarded as a combination of a carrier (e.g., pure sine wave) and a disturbance component imposed onto that waveform. The sinusoidal component is not the informative part in terms of an event detection or classification, but its existence perturbs some statistical parameters. Therefore, we remove sinusoidal component (also called stable limit circle, as shown in Fig.1b) during feature extraction procedure.

Fig.4 gives an example of a voltage sag processing procedure.

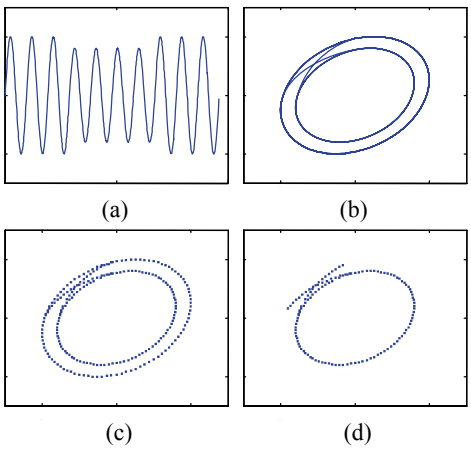

Fig.4 (a) Voltage sag waveform; (b) Voltage sag trajectory based on PSR; (c) Binary image of voltage sag trajectory; (d) Binary image of trajectory after carrier component being removed

2. Feature definition

Having illustrated the image processing procedure, we formulate the features extracted from characteristics carried by black pixels.

Definition 1 Carrier Component Similarity (CCS)

The binary image of disturbance trajectory is compared with stable limit cycle. A black pixel in disturbance trajectory is marked as Sinusoidal Pixel (SP) if a relevant point can be found in sine wave trajectory to satisfy

$$\sqrt{(x_i - x_j)^2 + (y_i - y_j)^2} \le \varepsilon, \tag{5}$$

where (x_i, y_i) are coordinates of the ith black pixel in disturbance trajectory, and (x_j, y_j) indicates the relevant pixel in stable limit cycle. ε is a small value greater than zero, considering ubiquitous noise.

CCS is defined as the number of SP:

$$CCS = n(\text{SP}). \tag{6}$$

Definition 2 Overlay Area (OA)

After removing previous SP, the rest black pixels describe how densely the disturbance component occupies the binary image. Hence *OA* is represented by the number of Remnant Pixels (RP):

$$OA = n(\text{RP}). \tag{7}$$

Definition 3 Mean Amplitude (MA)

The definition of *MA* is given as follows:

$$MA = \sum_{i=1}^{n(\text{RP})} \sqrt{x_i^2 + y_i^2} \Big/ n(\text{RP}), \tag{8}$$

where (x_i, y_i) are coordinates of the ith black pixel.

These definitions possess the ability to distinguish different disturbance patterns. Because of the oscillating envelope, each cycle of flicker waveform constructs a different trajectory in phase plane (as shown in Fig.3), so *OA* values of voltage flicker as well as flicker-related combined disturbances are much larger than those of other types. The carriers of harmonic disturbance are distorted (as shown in Fig.2), which results in smaller *CCS* value. Therefore, *CCS* is capable to indicate harmonic-related combined disturbances. *MA* implies the magnitude of disturbance event, so it is effective to distinguish among voltage sags and swells.

The next part gives the test results of these feature indices. The classification logic will be shown in Section 3.2.

3. Feature extraction diagram and results

Fig.5 shows the block diagram of PSR based feature extraction which consists of preprocessing, processing, and post-processing phases.

The patterns of combined disturbance studied in this paper include the harmonics combined with voltage sags and swells, as well as the flickers combined with sags and swells. The homologous single types are also taken into consideration.

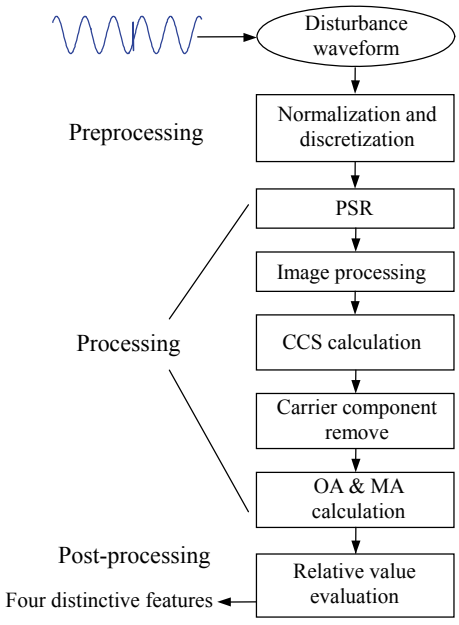

Fig.5 Diagram of PSR-based feature extraction

In order to uniform the disturbance feature expressions, the indices extracted will be divided by reference value obtained from standard sine wave. The scatter diagrams of normalized feature indices of the concerned disturbance patterns are presented in Fig.6.

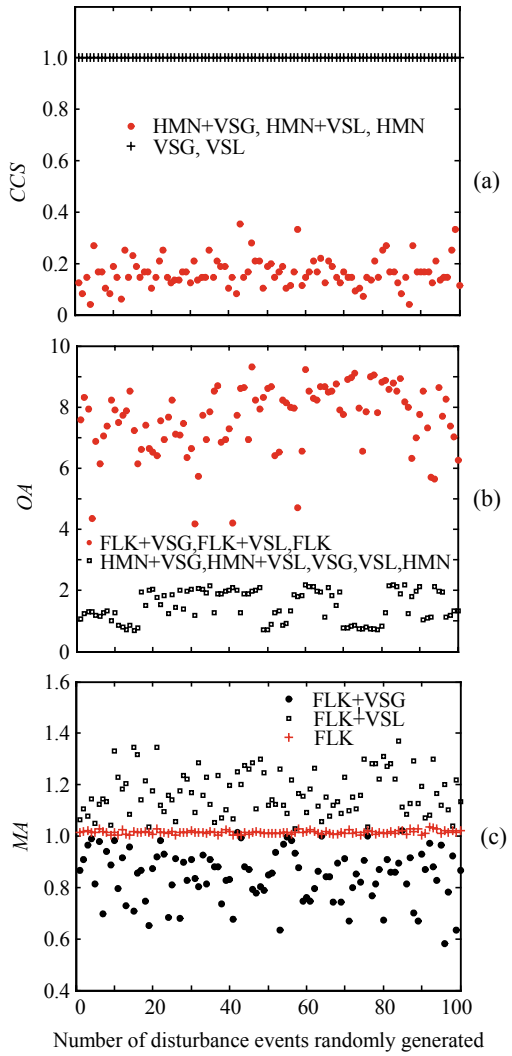

Fig.6 The scatter diagrams of disturbance features. HMN, FLK, VSG and VSL stand for harmonic, flicker, voltage sag and voltage swell, respectively. (a), (b) and (c) are the values of Carrier Component Similarity (CCS), Overlay Area (OA) and Mean Amplitude (MA), respectively

SVM-BASED AUTOMATIC RECOGNITION

Basic theory of SVM

SVM delivers the state-of-the-art performance in real applications, and is established as one of the standard tools for machine learning and data mining now. The basic objective is to find a hyperplane which best separates the positive/negative data in the feature space.

Considering a binary classification task with a set of linearly separable training samples $S=\{(x_1, y_1), \ldots, (x_n, y_n)\}$, where $\boldsymbol{x}$ is the input vector such that $\boldsymbol{x}\in\mathbb{R}^d$ (in d-dimensional input space) and y_i is the class label such that $y_i\in\{-1, 1\}$, the goal of training is to create a suitable discriminating function

$$f(\boldsymbol{x})=\langle \boldsymbol{w}\cdot\boldsymbol{x}\rangle+b, \tag{9}$$

where $\boldsymbol{x}$ is the input vector, $\boldsymbol{w}$ is the weight vector which determines the orientation of the hyperlane $f(\boldsymbol{x})=0$, and b is the bias or offset.

This function realizes data separation shown in Eq.(10) and maximizes the distance between the closest vector and the hyperplane.

$$\begin{cases}\langle \boldsymbol{w}\cdot\boldsymbol{x}_i\rangle+b\geq 1, & y_i=1,\\ \langle \boldsymbol{w}\cdot\boldsymbol{x}_i\rangle+b\leq -1, & y_i=-1,\end{cases} \quad i=1,2,\ldots,n. \tag{10}$$

For a linear SVM, the construction of discriminating function shown in Eq.(9) results in a convex optimization problem formed as

$$\min_{w,b}\frac{1}{2}\|\boldsymbol{w}\|^2,\ \text{s.t.}\ y_i\left(\langle \boldsymbol{w}\cdot\boldsymbol{x}_i\rangle+b\right)\geq 1,\ i=1,2,\ldots,n. \tag{11}$$

The minimization of linear inequalities is typically solved by the application of Lagrange duality theory. By introducing Lagrange multipliers α_i, Eq.(11) can be converted into

$$\begin{aligned}&\max_{\alpha} W(\boldsymbol{\alpha})=\sum_{i=1}^{n}\alpha_i-\frac{1}{2}\sum_{i,j=1}^{n}y_i y_j\alpha_i\alpha_j\langle \boldsymbol{x}_i\cdot\boldsymbol{x}_j\rangle,\\ &\text{s.t.}\quad \sum_{i=1}^{n}y_i\alpha_i=0,\quad \alpha_i\geq 0,\quad i=1,2,\ldots,n.\end{aligned} \tag{12}$$

According to Karush-Kuhn-Tucker (KKT) condition, solutions $\boldsymbol{\alpha}^*$, $(\boldsymbol{w}^*, b^*)$ must satisfy:

$$\alpha_i^*\left[y_i\left(\langle \boldsymbol{w}^*\cdot\boldsymbol{x}_i\rangle+b^*\right)-1\right]=0,\quad i=1,2,\ldots,n. \tag{13}$$

The samples which correspond to $\alpha_i^*\neq 0$ are support vectors. These points lie on the hyperplane

and affect the decision of the machine. Finally the relevant classifier function becomes

$$f(\boldsymbol{x}) = \operatorname{sgn}\left[\sum_{i=1}^{n} \alpha_i^* y_i x_i \cdot \boldsymbol{x} + b^*\right]. \quad (14)$$

Classifier design

A single SVM is constructed to respond binary to the testing data. It has to be augmented with other strategies to achieve multi-case classification. We utilized a layered clustering idea to construct SVM classifier. First, the set of all PQ cases is divided into two subsets according to similarities among cases by a single SVM. Then, these two subsets are divided into four smaller sets. Totally seven SVMs are needed to separate different cases until each set contains only one PQ pattern. The sorting logic is shown in Fig.7, in which the texts in square brackets indicate the candidates for analysis, and the features in parentheses are the inputs to the corresponding SVM.

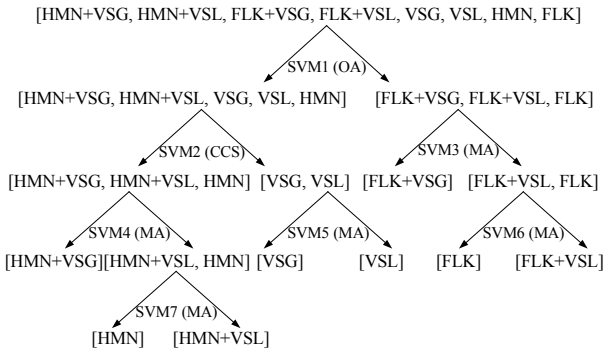

Fig.7 Tree diagram of the sorting logic

It is much clear to take SVM1 as an example to illustrate. As shown in Fig.6b, *OA* values of flicker-combined disturbances are always greater than those of other disturbances. So *OA* is chosen as the input feature of SVM1, and through SVM1, flicker-related combined cases as well as flickers are excluded from other samples. By proceeding iteratively, all kinds of disturbances will be recognized one by one.

SIMULATION AND ANALYSIS

Data generation

To obtain representative signals that possess the inherent characteristics of most common PQ disturbances, disturbance signals are initially generated in MATLAB 7.0. Some unique attributes for each disturbance are allowed to change randomly, within specified limits, in order to create different disturbance cases. The randomness in the generated signals is intended to test the universal validity of classification system proposed in this paper.

The aforementioned eight categories of disturbances are simulated based on ten cycles of voltage waveform. These waveforms are generated at a sampling rate of 96 samples per cycle for a total of 960 points.

Table 1 provides a detailed summary of disturbance signal models and their controlled parameters. One hundred and sixty training samples and 1600 testing samples with different parameters were generated and utilized (20 training samples and 200 testing samples for each category).

Table 1 Power quality disturbance signal models of PSR-based feature extraction

PQ disturbances	Models	Controlled parameters
HMN+VSG	$x(t)=A[\sin(\omega t)+\alpha_3\sin(3\omega t)+\alpha_5\sin(5\omega t)]\times\{1-\alpha[u(t-t_1)-u(t-t_2)]\}$	$0.1\le\alpha\le0.9$, $T\le t_2-t_1\le8T$ $0.1\le\alpha_3\le0.2$, $0.05\le\alpha_5\le0.1$
HMN+VSL	$x(t)=A[\sin(\omega t)+\alpha_3\sin(3\omega t)+\alpha_5\sin(5\omega t)]\times\{1+\alpha[u(t-t_1)-u(t-t_2)]\}$	$0.1\le\alpha\le0.5$, $T\le t_2-t_1\le8T$ $0.1\le\alpha_3\le0.2$, $0.05\le\alpha_5\le0.1$
FLK+VSG	$x(t)=A[1+\beta\sin(\gamma\omega t)\sin(\omega t)]\times\{1-\alpha[u(t-t_1)-u(t-t_2)]\}$	$0.1\le\alpha\le0.9$, $T\le t_2-t_1\le8T$ $0.1\le\beta\le0.2$, $0.1\le\gamma\le0.2$
FLK+VSL	$x(t)=A[1+\beta\sin(\gamma\omega t)\sin(\omega t)]\times\{1+\alpha[u(t-t_1)-u(t-t_2)]\}$	$0.1\le\alpha\le0.5$, $T\le t_2-t_1\le8T$ $0.1\le\beta\le0.2$, $0.1\le\gamma\le0.2$
VSG	$x(t)=A\{1-\alpha[u(t-t_1)-u(t-t_2)]\}\sin(\omega t)$	$0.1\le\alpha\le0.9$, $T\le t_2-t_1\le8T$
VSL	$x(t)=A\{1+\alpha[u(t-t_1)-u(t-t_2)]\}\sin(\omega t)$	$0.1\le\alpha\le0.5$, $T\le t_2-t_1\le8T$
HMN	$x(t)=A[\sin(\omega t)+\alpha_3\sin(3\omega t)+\alpha_5\sin(5\omega t)]$	$0.1\le\alpha_3\le0.2$, $0.05\le\alpha_5\le0.1$
FLK	$x(t)=A[1+\beta\sin(\gamma\omega t)\sin(\omega t)]$	$0.1\le\beta\le0.2$, $0.1\le\gamma\le0.2$

HMN, FLK, VSG and VSL stand for harmonic, flicker, voltage sag and voltage swell, respectively

Simulation results

We used 160 training samples to optimize the parameters of the SVMs shown in Fig.7, and other 1600 testing samples to test the feasibility of classifier. The simulation procedures are analyzed by using MATLAB that runs on a personal computer along with Athlon 1.69 GHz processor and 512 MB memory. Table 2 presents the simulation results.

It can be found that the constructed and trained SVM classifier results in a satisfying classification rate of 98.5% with input features extracted using PSR. In order to evaluate performance of the proposed system, we carried out comparative tests using WT and ANN, which are reported blow.

Comparative tests

WT is efficient in feature extraction of single PQ disturbance. Based on WT and discrete wavelet multiresolution analysis, different features were chosen to construct the feature vectors for subsequent training and testing in previous works. We adopted 11-dimensional features which carry energy information at each decomposition level proposed in (He and Starzyk, 2006). In order to have a fair result comparison, four commonly used wavelet families, named Haar wavelet, Daubechie's wavelet (Db for short), Symlets and Coiflets wavelets (Sym and Coif for short, respectively), are taken into account. Table 3 shows the classification results using the combination of WT-based feature extraction and SVM classifier. It can be found that Sym6 wavelet results in a relatively high accuracy. So we changed decomposition level with Sym6 wavelet for further research. Fig.8 shows the relationship between the decomposition level and classification performance. Table 4 illustrates more details about the best classification performance at level 9.

ANN is widely viewed as having a desirable topology for PQ disturbance recognition. The pattern of ANN utilized here is BP network with 3 layers. The numbers of input and output layer nodes are 3 and 8,

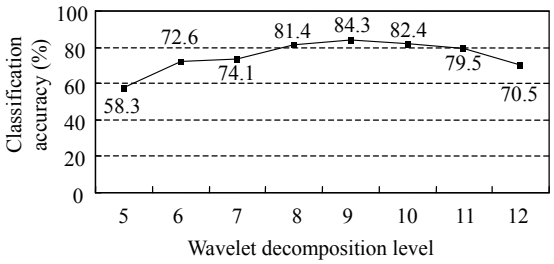

Fig.8 Classification accuracy with Sym6 wavelet at different decomposition levels

Table 2 Classification results of the system proposed in this paper (based on PSR and SVM)

PQ disturbance patterns	Classification results								Calculation time (s)
	HMN+VSG	HMN+VSL	FLK+VSG	FLK+VSL	VSG	VSL	HMN	FLK	
HMN+VSG	192	0	0	0	0	0	8	0	25.0
HMN+VSL	0	199	0	0	0	0	1	0	26.8
FLK+VSG	1	0	194	0	0	0	0	5	25.5
FLK+VSL	0	0	0	194	0	0	0	6	20.6
VSG	0	0	0	0	200	0	0	0	23.3
VSL	0	0	0	0	0	200	0	0	23.6
HMN	0	0	0	0	0	0	200	0	26.5
FLK	0	0	1	2	0	0	0	197	20.3
Average results	Classification accuracy: 98.5%								24.0

HMN, FLK, VSG and VSL stand for harmonic, flicker, voltage sag and voltage swell, respectively

Table 3 Classification results of the system based on WT and SVM

Wavelet	Average accuracy (%)	Calculation time (s)	Wavelet	Average accuracy (%)	Calculation time (s)	Wavelet	Average accuracy (%)	Calculation time (s)
Haar	68.6	19.3	Db9	63.4	20.5	Sym8	78.9	18.0
Db2	73.5	21.2	Db10	69.4	19.4	Coif1	82.3	19.2
Db3	73.4	18.7	Sym2	73.3	20.6	Coif2	75.0	20.1
Db4	70.1	21.1	Sym3	72.6	19.5	Coif3	67.7	19.3
Db5	64.1	21.0	Sym4	79.8	19.3	Coif4	64.5	18.7
Db6	64.8	20.2	Sym5	80.6	19.1	Coif5	60.3	19.2
Db7	71.4	21.2	**Sym6**	**82.4**	**19.1**			
Db8	68.7	20.7	Sym7	78.6	18.9			

Table 4 Confusion matrix about classification performance with Sym6 wavelet at decomposition level 9

PQ disturbance patterns	Classification results								Calculation time (s)
	HMN+VSG	HMN+VSL	FLK+VSG	FLK+VSL	VSG	VSL	HMN	FLK	
HMN+VSG	186	5	0	0	0	0	9	0	16.0
HMN+VSL	0	191	0	0	0	0	9	0	15.9
FLK+VSG	0	1	118	0	67	0	0	14	22.5
FLK+VSL	0	0	0	124	0	55	0	21	20.4
VSG	0	0	9	0	184	0	0	7	20.3
VSL	0	0	0	24	0	158	0	18	20.5
HMN	9	0	0	0	0	0	191	0	16.0
FLK	0	0	2	0	0	1	0	197	20.9
Average results	Classification accuracy: 84.3%								19.1

HMN, FLK, VSG and VSL stand for harmonic, flicker, voltage sag and voltage swell, respectively

respectively, which correspond to the dimension of PSR-based feature and the number of disturbance patterns. The number of hidden layer nodes is scanned from 3 to 12. For each run, the ANN was trained with 5000 iterations. Fig.9 shows the results using combination of PSR and ANN classifier.

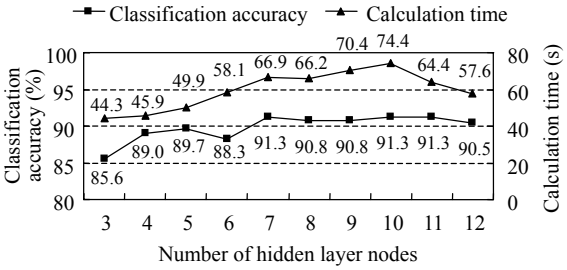

Fig.9 Classification results of the system based on PSR and ANN

Discussion

Table 3 and Fig.8 show the classification performance based on WT and SVM classifier with different wavelets and different decomposition levels. It can be found that the highest classification accuracy among these tests is 84.3%, which is lower than that obtained by the system proposed in this paper with PSR-based features.

From Table 4, it can be seen that the feature vectors obtained by WT are not suitable for recognition of flicker-related combined disturbances. This is because in the condition of a relatively low frequency of modulating wave, the energy distribution of flicker is closely similar to that of voltage swell. In other words, the spectral characteristics in frequency domain of flicker, swell and flicker-combined disturbances are not so "unique" as visually presented waveforms in time domain. Therefore, PSR-based image analysis and feature extraction processed in time domain results in higher classification accuracy.

Fig.9 shows the results based on PSR and ANN classifier. An average recognition rate of about 91% is stably achieved while the number of hidden layer nodes changes from 7 to 12. This accuracy is acceptable but still lower. Besides, ANN inherently requires a large number of training cycles and hence a longer calculation time, which is also proved in this study.

In a word, the advantage of the classification system proposed in this paper is its high recognition rate for PQ combined disturbances and high training speed.

CONCLUSION

The classification of Power Quality (PQ) disturbance events is an important task for precise monitoring and analysis of distribution systems. With the overspread of long-term harmonic or flicker disturbances, the relevant combined disturbance patterns should be taken into consideration. This paper introduces a novel classification system which can achieve satisfying classification accuracy for several PQ combined disturbances and their homologous single patterns.

This system consists of two parts: a PSR-based feature extraction and an SVM classifier. The function of the former is to extract features from disturbance signals, and the latter is to recognize and classify different types of power disturbances. Several typical disturbances are taken into consideration. The evaluation results with 160 training samples and 1600

testing samples demonstrate that the proposed method can effectively classify different kinds of PQ combined disturbances.

Comparative studies further show the advantages of this system. PSR-based feature vectors preferably carry unique characteristics of different PQ patterns, especially flicker-related combined disturbances. Linear SVM classifier function is computationally much simpler. Hence, a classification system using PSR and SVM achieves better performance than some existing techniques. In addition, the idea of combining PSR with SVM classifier could potentially be used in other domains, such as audio data analysis, automatic target recognition, etc.

References

Abdel-Galil, T.K., El-Saadany, E.F., Youssef, A.M., Salama, M.M.A., 2005. Disturbance classification using hidden Markov models and vector quantization. *IEEE Trans. on Power Delivery*, **20**(3):2129-2135. [doi:10.1109/TPWRD.2004.843399]

Axelberg, P.G.V., Irene, Y.H.G., Bollen, M.H.J., 2007. Support vector machine for classification of voltage disturbances. *IEEE Trans. on Power Delivery*, **22**(3):1297-1303. [doi:10.1109/TPWRD.2007.900065]

Chen, S., 2005. Feature selection for identification and classification of power quality disturbances. IEEE Power Engineer Society General Meeting, **3**:2301-2306. [doi:10.1109/PES.A82005.1489187]

Chilukuri, M.V., Dash, P.K., 2004. Multiresolution S-transform-based fuzzy recognition system for power quality events. *IEEE Trans. on Power Delivery*, **19**(1):323-330. [doi:10.1109/TPWRD.2003.820180]

Chilukuri, M.V., Dash, P.K., Basu, K.P., 2004. Time-Frequency Based Pattern Recognition Technique for Detection and Classification of Power Quality Disturbances. IEEE Region 10 Conf., **3**:260-263. [doi:10.1109/TENCON.2004.1414756]

Gaouda, A.M., Kanoun, S.H., Salama, M.M.A., 2001. On-line disturbance classification using nearest neighbor rule. *Electr. Power Syst. Res.*, **57**(1):1-8. [doi:10.1016/S0378-7796(00)00120-6]

Germen, E., Ece, D.G., Gerek, Ö.N., 2005. Self organizing map (SOM) approach for classification of power quality events. *LNCS*, **3696**:403-408.

He, H.B., Starzyk, J.A., 2006. A self-organizing learning array system for power quality classification based on wavelet transform. *IEEE Trans. on Power Delivery*, **21**(1):286-295. [doi:10.1109/TPWRD.2005.852392]

Li, Z.Y., Wu, W.L., 2006. Detection and Identification of Power Disturbance Signals Based on Nonlinear Time Series. IEEE 6th World Congress on Intelligent Control and Automation, **9**:7646-7650. [doi:10.1109/WCICA.2006.1713454]

Li, Z.Y., Wu, W.L., 2007. Phase space reconstruction based classification of power disturbances using support vector machines. *LNCS*, **4426**:680-687.

Liao, Y., Lee, J.B., 2004. A fuzzy-expert system for classifying power quality disturbances. *Int. J. Electr. Power & Energy Syst.*, **26**(3):199-205. [doi:10.1016/j.ijepes.2003.10.012]

Tiwari, A.K., Shukla, K.K., 2002. Wavelet transform based fuzzy inference system for power quality classification. *LNCS*, **2257**:148-155.

Tong, W.M., Song, X.L., Zhang, D.Z., 2006. Recognition and classification of power quality disturbances based on self-adaptive wavelet neural network. *LNCS*, **3972**:1386-1394.

Wang, M., Mamishev, A.V., 2004. Classification of power quality events using optimal time-frequency representations. *IEEE Trans. on Power Delivery*, **19**(3):1488-1503. [doi:10.1109/TPWRD.2004.829940]

Youssef, A.M., Abdel-Galil, T.K., El-Saadany, E.F., Salama, M.M.A., 2004. Disturbance classification utilizing dynamic time warping classifier. *IEEE Trans. on Power Delivery*, **19**(1):272-278. [doi:10.1109/TPWRD.2003.820178]